

Complex Order $PI^{\alpha+j\beta}D^{\gamma+j\theta}$ Design for Surface Roughness Control in Machining CNT Al-Mg Hybrid Composites

Ravi Sekhar^{*1}, Tejinder Paul Singh², Pritesh Shah¹

¹Symbiosis Institute of Technology (SIT), Symbiosis International (Deemed University) (SIU), Pune, 147001, India

²Department of Mechanical Engineering, Thapar Institute of Engineering & Technology, Patiala, 111045, India

ARTICLE INFO

Article history:

Received: 28 August, 2020

Accepted: 01 November, 2020

Online: 08 November, 2020

Keywords:

Complex order controller

Fractional calculus

Fractional order controller

Nano composites

Carbon nanotubes

Fractional modeling

Bode diagram

ABSTRACT

Accurate machining control is indispensable for the smart factories of tomorrow. Variations in controller responses may cause unacceptable process deviations during machining leading to productivity losses and possible damage. In the present work, a complex order $PI^{\alpha+j\beta}D^{\gamma+j\theta}$ (COPID) controller was designed to effectively control surface roughness generation while machining CNT Al-Mg hybrid composites. Performance of the designed complex order controller was compared against the conventional PID and fractional order PID (FOPID) controllers for the machined surface roughness system. Output signal responses indicate that the complex order controller attains the desired surface roughness set point with zero percent overshoot in almost same settling time (46 sec) as PID (41 sec) and FOPID (46 sec) controllers. The PID and FOPID output signals registered overshoots of 96.8 % and 36.7 % respectively. Similarly, in case of control signals (feed rate) the COPID controller successfully minimised peak overshoot to 4.6 %; as compared to 64.2 % and 96.5 % in case of the PID and FOPID controllers respectively. The COPID controller was also effective in reducing its peak time response metric (2.001 % for control signal and no peak time for output signal due to zero overshoot). In comparison, the PID and FOPID controllers recorded higher response peak times (7 sec / 26 sec for the PID output/control and 5 sec / 7.84 sec for FOPID output/control signal responses). Overshoot elimination in output signal (surface roughness) is crucial for consistency of the machined surface quality. Similarly, overshoot minimisation in control signal (feed rate) is critical because excessive feed rate can damage the cutting tool, work piece, machinery and is a potential safety hazard for the machine operator as well. Hence, the COPID controller can be safely and extensively applied in smart industrial control systems of the future.

1 Introduction

This paper is an extension of the work originally reported in the 2019 IEEE International Conference on Mechatronics, Robotics and Systems Engineering (MoRSE) [1]. In that work, firstly the multi input single output system of surface roughness generation during machining of the CNT Al-Mg composites was identified using the ARX and ARMAX model structures. Thereafter, the fractional order PID (FOPID) controller was designed to control the identified system at the desired set point (surface roughness). The authors reported that the ARMAX model based FOPID control exhibited better time domain characteristics as compared to the ARX model based FOPID controller design. The current work extends this work further to include complex order controller design to improve the

time domain performance even more. PID controller has also been implemented for better comparisons. Moreover, the output signal time domain specifications corresponding to the machining variables not discussed in the previous work have also been included in the present study.

Metal matrix composites are new age materials finding new and varied applications due to their superior mechanical properties over conventional alloys [2]. Carbon nanotubes (CNT) in particular have attracted attention of researchers worldwide owing to the superior strengthening characteristics imparted by these nano sized particles to the base metal alloys [3]. Aluminum based alloy systems have almost a universal presence across industry sectors and products [4]. Combination of carbon nanotubes and aluminum-magnesium alloys results in composites with superior mechanical characteristics.

*Corresponding Author: Ravi Sekhar, Symbiosis Institute of Technology, Pune, India Contact No. +91 20 28116400 & Email ravi.sekhar@sitpune.edu.in

Modeling and designing effective controllers is an important step towards automating the machining of these modern materials.

Generally, PID controllers find extensive applications due to their ease of implementation and maintenance in industrial systems. However, specialized machinery may require more sophisticated controllers having better design characteristics. Fractional order controllers offer a better design alternative because they have two more parameters to tune as compared to the traditional PID controllers [5, 6]. These controllers are based on fractional calculus, a branch of integral calculus that enables fractional orders of the model structure parameters. Fractional order PID controllers (FOPID) have been demonstrated to exhibit better performance characteristics in various application areas such as control systems, signal processing, medical research, material science and many more [7]–[10]. FOPID controllers prove to be more robust against system variations against their PID counterparts. Therefore, FOPID controllers are being increasingly preferred in more dynamic systems across industries [11]–[14]. Machining of complex materials like the metal matrix composites is one such example of a dynamic system; wherein the material composition is anisotropic and calls for a more robust controller architecture [6].

Complex order PID (COPID) controllers are the next step in the controller evolution [15]. They are an extension of the FOPID controllers just as the FOPID are extended versions of the PID controllers. The COPID have further two parameters to tune over the FOPID controllers. In the recent years, COPID controllers have been gradually attracting increasing investigations into their design and application aspects [16]–[18]. Khandani et al [19] designed a complex order controller for DC motors. Pinto and Carvalho [20] derived a complex order model for HIV infection drug resistance. Machado [18] optimized complex order controller for linear and non linear systems using genetic algorithm. Ayadi and Amairi [21] applied numerical optimization to tune complex order controller for a second order time delay resonant system. Hanif et al [22] implemented genetic algorithm for tuning of complex order controller design. Silva et al [23] applied complex order structure to model hexapod robot locomotion based on foot-ground transfer function. Jacob et al [15] reviewed frequency domain, time domain and stability aspects in complex order modeling of linear systems. Tare et al [24] compared integral, fractional and complex order controller performances for fractional order systems. Adams et al [25] determined the transfer function solution to the complex order differential equation. Shahiri et al [26] investigated robust control of a non linear fuel cell system using complex order architecture. From the literature review, it appears that the application of COPID controller in machining systems needs attention. The current work aims to bridge this gap.

The CNT Al-Mg composite experimental details may be referred to in the previous part [1] of the current work. It involved variation of the input machining parameters (cutting speed, feed and depth of cut) and data collection of the corresponding values of the machined surface roughness. Machining experiments were performed on a CNC turning center (Simple Turn 5057 Haas Automation) using chemical vapour deposition (CVD) coated tool inserts (Seco CNMG120408). Surface roughness was measured by a Handy Surf E-DTS570 tester. The best performing model structure (ARMAX) describing this machined surface roughness

system in the previous work was adopted in the current study for the COPID and PID controller design. The FOPID controller time domain characteristics from the previous work [1] were referred to in the current work for comparisons with the COPID and PID controller responses. In the previous work, high peak overshoots were detected in output / control signal responses of the FOPID controller. The current study aimed to minimise / eliminate peak overshoots by employing COPID controller design. The following section details upon the design methodologies followed for the implementation of the PID, FOPID and COPID controllers in composite material machined surface roughness system.

2 Controller Design Methodology

This section describes the design methodologies of the PID, FOPID and COPID controllers for the machined surface roughness system. All controllers were designed to attain output set point of 1 micron surface roughness. In machining, cutting speed is inversely related to surface roughness whereas depth of cut directly increases machined surface roughness levels. However, feed rate has the most significant effect on surface roughness generation [2]. Therefore, feed rate parameter was selected as the manipulated variable in the current study whereas cutting speed and depth of cut were maintained at their mid levels as per the experimental design [1]. Thus, all controllers were designed to control this multi input (cutting speed, feed, depth of cut) and single output (surface roughness) system as shown in Figure 1.

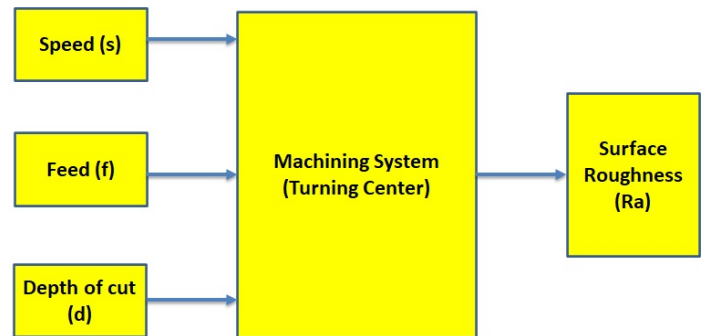


Figure 1: Multi input single output system schematic for the nano composite machined surface roughness system

2.1 PID controller

The PID controller has been widely implemented in industries since many years because of its simple structure and compatibility with the industrial automation software [27]. In the current work, Simulink block was utilised to implement PID controller for the machined surface roughness plant. The PID controller structure is given as follows:

$$C(s) = K_P + K_I \left(\frac{1}{s} \right) + K_D \left(\frac{N}{1 + N \frac{1}{s}} \right) \quad (1)$$

where, K_P is the proportional gain, K_I is the integral gain, K_D is derivative gain and N is the filter coefficient of derivative. The PID block was auto tuned in Simulink using the time domain approach.

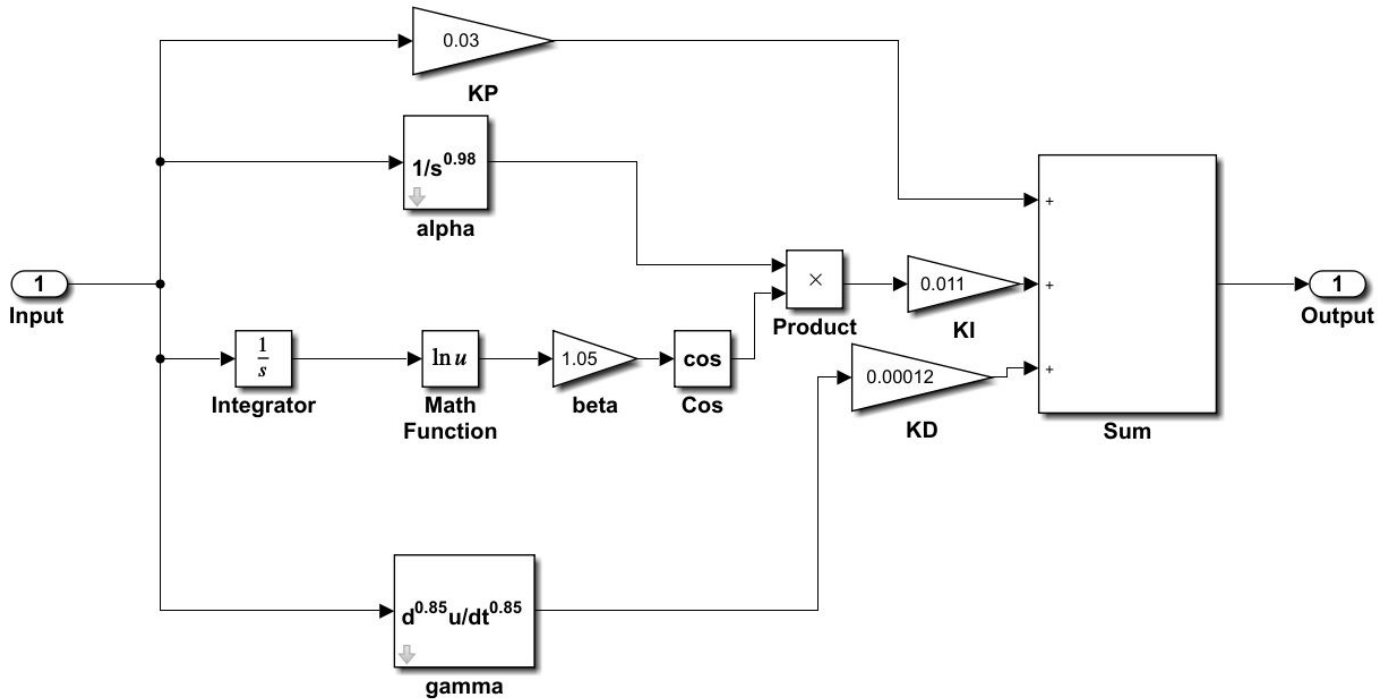


Figure 2: Complex $PI^{\alpha+j\beta}D^{\gamma+j\theta}$ Controller Structure in Simulink

2.2 FOPID controller

Fractional PID (FOPID) controller is an extension of the classical PID controller and is designed based on fractional calculus [28]. In this controller, the orders of integration and derivation are real numbers [29, 14]. The FOPID controller has the following controller structure:

$$C(s) = K_P + K_I \left(\frac{1}{s}\right)^\lambda + K_D s^\mu \quad (2)$$

where μ is the order of derivative and λ is the order of integration. There are five parameters in the fractional PID controller. This controller has the property of isodamping making it more robust against variations in the system parameters. The values of λ and μ were taken between 0 to 2 for the closed loop system to be stable.

Following equations were employed to synthesise the fractional calculus for the fractional PID controller application:

$$\begin{aligned} \omega_u &= \sqrt{\omega_h \omega_b} \\ \omega'_0 &= \alpha^{-0.5} \omega_u; \omega_0 = \alpha^{0.5} \omega_u; \\ \frac{\omega'_{k+1}}{\omega'_k} &= \frac{\omega_{k+1}}{\omega_k} = \alpha \eta > 1 \\ \frac{\omega'_{k+1}}{\omega_k} &= \eta > 0; \frac{\omega_k}{\omega'_k} = \alpha > 0 \end{aligned}$$

$$N = \frac{\log(\omega_N/\omega_0)}{\log(\alpha\eta)}$$

where, N is the order of approximation, ω_h and ω_b are the frequency bounds for approximation.

In the present work, FOMCON toolbox was used for implementation of FOPID and COPID controllers [12]. In this toolbox, Simulink blocks are available for various applications of fractional calculus. It can be used for designing controllers in continuous/discrete time scales, fractional order state space and many more. In FOPID design, the derivative action was considered zero ($K_D = 0$ and $\mu = 0$). The other gain parameters are taken from PID controller settings. Value of λ was selected based on the approach given by Shah and Agashe [29].

2.3 COPID controller

Complex order PID (COPID) controller idea originated from the 3rd generation of CRONE controller [30, 11]. COPID controller is similar to FOPID controller except that the orders of integration and derivation are complex instead of real numbers. The COPID controller has the following structure [16, 26].

$$C(s) = K_P + K_I \left(\frac{1}{s}\right)^{\alpha+j\beta} + K_D (s)^{\gamma+j\theta} \quad (3)$$

where, K_P is the proportional gain, K_I is the integral gain, K_D is derivative gain and $\alpha, \beta, \gamma, \theta$ are the orders of the complex order controller.

To implement the above equation, a simplification procedure was carried out in two steps. Firstly, the complex integration was written as:

$$K_I \left(\frac{1}{s}\right)^{\alpha+j\beta} = K_I \left(\frac{1}{s}\right)^\alpha \left(\frac{1}{s}\right)^{j\beta}$$

$$K_I \left(\frac{1}{s}\right)^{\alpha+j\beta} = K_I \left(\frac{1}{s}\right)^\alpha * e^{\ln\left(\frac{1}{s}\right)^{j\beta}}$$

$$K_I \left(\frac{1}{s}\right)^{\alpha+j\beta} = K_I \left(\frac{1}{s}\right)^\alpha * e^{j\beta \ln\left(\frac{1}{s}\right)}$$

$$K_I \left(\frac{1}{s}\right)^{\alpha+j\beta} = K_I \left(\frac{1}{s}\right)^\alpha * \left[\cos\left(\beta \ln\left(\frac{1}{s}\right)\right) + j \sin\left(\beta \ln\left(\frac{1}{s}\right)\right) \right]$$

The imaginary part of the above equation cannot be synthesised for time domain implementation of the system. Hence, for implementing the COPID controller in Simulink, imaginary part of the above equation was omitted [16].

$$K_I \left(\frac{1}{s}\right)^{\alpha+j\beta} = K_I \left(\frac{1}{s}\right)^\alpha * \left[\cos\left(\beta \ln\left(\frac{1}{s}\right)\right) \right] \quad (4)$$

Similarly, derivative component of the Eq. (3) was simplified for implementation as follows -

$$K_D * s^{\gamma+j\theta} = K_D * s^\gamma * s^{j\theta}$$

$$K_D * s^{\gamma+j\theta} = K_D * s^\gamma * e^{\ln s^{j\theta}}$$

$$K_D * s^{\gamma+j\theta} = K_D * s^\gamma * e^{j\theta \ln s}$$

$$K_D * s^{\gamma+j\theta} = K_D * s^\gamma * [\cos(\theta \ln s) + j \sin(\theta \ln s)]$$

The imaginary part of the above equation cannot be synthesised for time domain implementation of the system. Hence, for implementing the COPID controller in Simulink, imaginary part of the above equation was omitted [16].

$$K_D * s^{\gamma+j\theta} = K_D * s^\gamma * [\cos(\theta \ln(s))] \quad (5)$$

Combining Eq. (4) and (5), the COPID controller structure may be rewritten as

$$C(s) = K_P + K_I \left(\frac{1}{s}\right)^\alpha * \left[\cos\left(\beta \ln\left(\frac{1}{s}\right)\right) \right] + K_D * s^\gamma * [\cos(\theta \ln(s))] \quad (6)$$

The COPID controller given in Eq. (6) was initially tuned by incorporating the reference values of FOPID controller and was further fine tuned based on the principles given in literature [31, 29]. The fine tuned COPID controller was implemented in Simulink (Matlab) as shown in figure 2. The initial value of integer order integrator was assumed to be a small number during the controller implementation.

3 Results and Discussions

This section describes the different controller structures, output / control signal responses, time domain characteristics and Bode plot

for the COPID controller. The discrete-time ARMAX model (order 3331) with 1 sec sample time from the previous work [1] was obtained as follows:

$$A(z)y(t) = B(z)u(t) + C(z)e(t)$$

$$A(z) = 1 - 0.3675z^{-1} + 0.4876z^{-2} - 0.3772z^{-3}$$

$$B_1(z) = -0.001019z^{-1} - 0.003656z^{-2} + 0.01446z^{-3}$$

$$B_2(z) = 0.6741z^{-1} + 0.2097z^{-2} + 13.82z^{-3}$$

$$B_3(z) = -1.569z^{-1} + 0.4574z^{-2} - 1.532z^{-3}$$

$$C(z) = 1 + 0.4142z^{-1} + 0.554z^{-2} - 0.4004z^{-3}$$

This model depicts the CNT Al-Mg composite machined surface roughness system considered in the current study. The PID controller applied on this model structure has the following structure:

$$C(s) = 0.0407 + 0.0143 \frac{1}{s} - 0.0633 \frac{0.4367}{1 + 0.4367 \frac{1}{s}} \quad (7)$$

The output and control signal responses of this PID controller for a set point of 1 micron surface roughness are shown in Fig. 3 and Fig. 4 respectively.

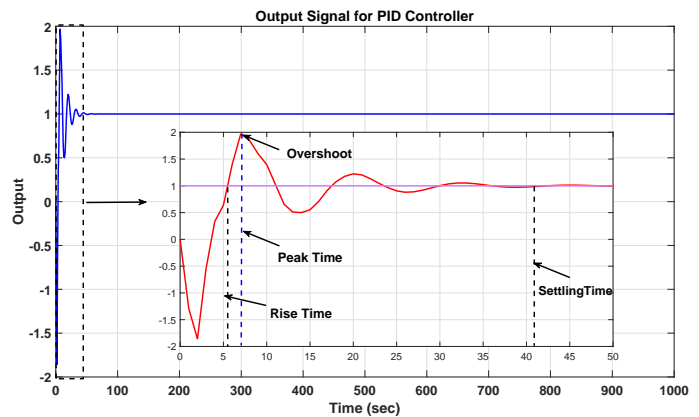


Figure 3: PID controller output (surface roughness, μ) for the machined surface roughness system

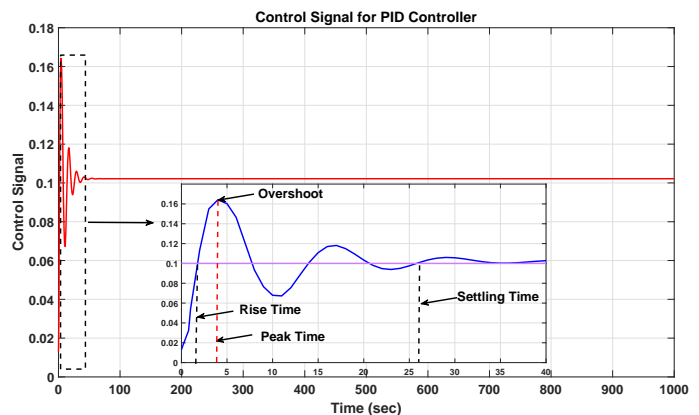


Figure 4: PID control signal (feed rate, mm / rev) for the machined surface roughness system

Following is the structure of the FOPID controller applied to the

composite machined surface roughness system -

$$C(s) = 0.0407 + 0.0143 \frac{1}{s^{0.952}} \quad (8)$$

Fig. 5 and Fig. 6 depict the output and control signal plots for the FOPID controller set at 1 micron surface roughness output.

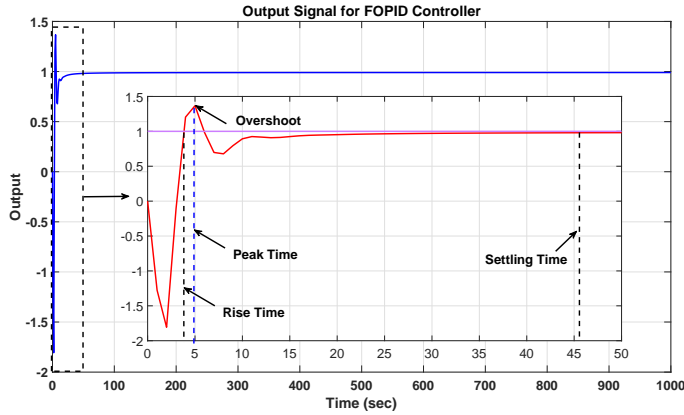


Figure 5: Fractional PID controller output (surface roughness, μ) for the machined surface roughness system

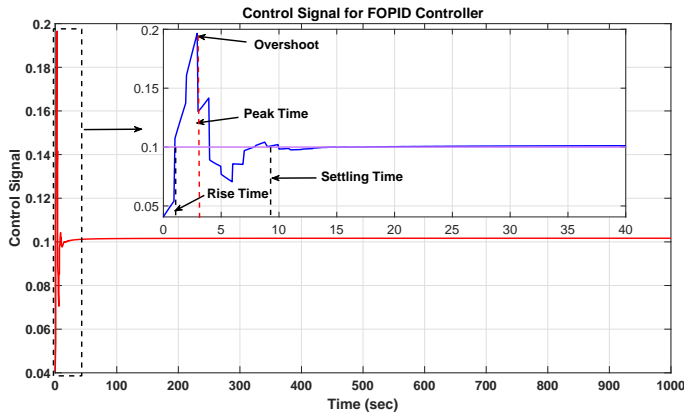


Figure 6: Fractional PID control signal (feed rate, mm / rev) for the machined surface roughness system

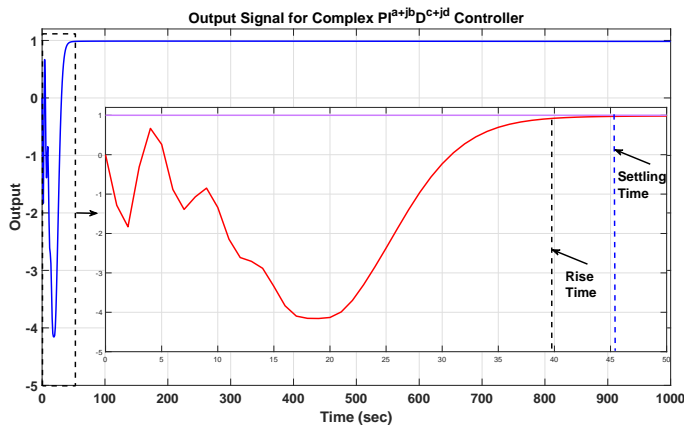


Figure 7: Complex $PI^{\alpha+\beta}D^{\gamma+\delta}$ controller output (surface roughness, μ) for the machined surface roughness system

The complex order controller structure for the same system is shown below -

$$C(s) = 0.03 + 0.011 \frac{1}{s^{0.98+j1.05}} + 0.00012s^{0.85+j0} \quad (9)$$

The output and control signal trends for the COPID controller are shown in Fig. 7 and Fig. 8 respectively.

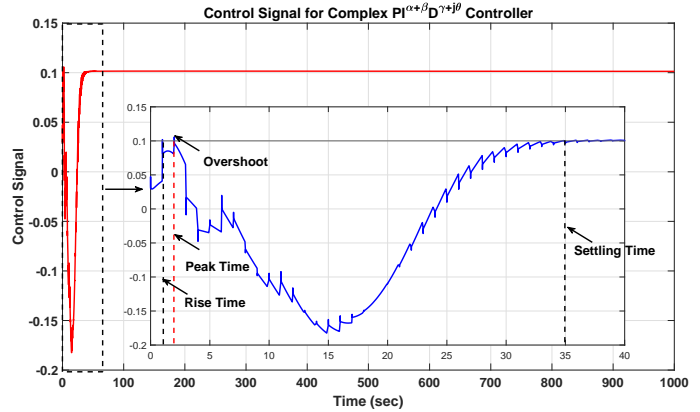


Figure 8: Complex $PI^{\alpha+\beta}D^{\gamma+\delta}$ control signal (feed rate, mm / rev) for the machined surface roughness system

Table 1: Time domain specifications of output signals

	PID	FOPID	COPID
Rise Time (sec)	5	3.8	39
Peak Time (sec)	7	5	NA
Settling Time (sec)	41	46	46
Overshoot (%)	96.8	36.7	0

Table 2: Time domain specifications of control signals

	PID	FOPID	COPID
Rise Time (sec)	2	1	1
Peak Time (sec)	4	2.924	2.001
Settling Time (sec)	26	7.844	34.38
Overshoot (%)	64.2	96.5	4.6

Table 1 shows the output signal (surface roughness) time domain specifications of the PID, FOPID and COPID controllers for the machined composite surface roughness system. The PID controller scores slightly better than the FOPID and COPID controllers in case of response settling time. PID also scores significantly better than the COPID controller in terms of the rise time. FOPID controller attains the least rise time. However, the COPID controller positively removes peak overshoot from the output signal. The other two controllers have high overshoots in their respective output signal responses. High overshoot in the surface roughness output is undesirable from quality perspective. Generally, critical industrial components require tight dimensional and surface roughness tolerances. Hence, for such cases of precision manufacturing, complex

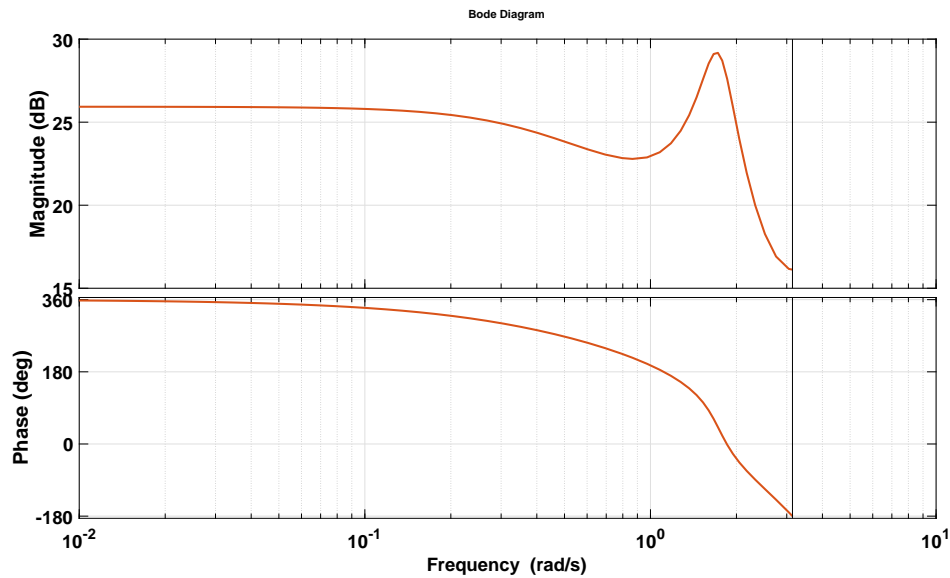


Figure 9: Bode plot for complex order controller

order controller promises to be a better alternative over PID and FOPID controllers.

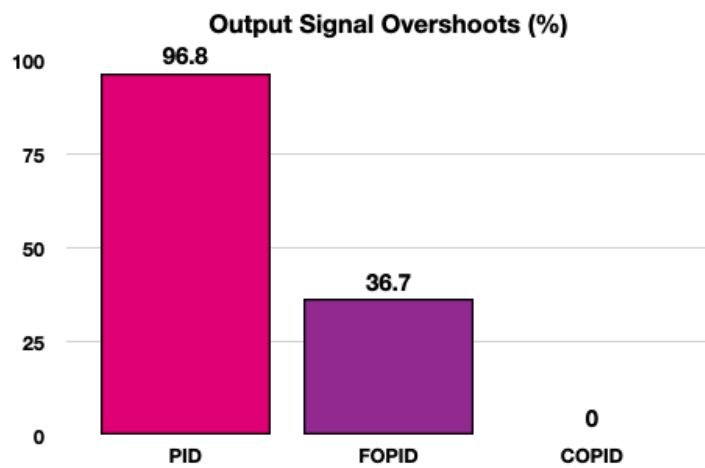


Figure 10: Output Signal Overshoots (%)

Table 2 shows the time domain characteristics of the control signal (feed rate) responses. In this case, the FOPID controller performs well in terms of the rise and settling times. The COPID outperforms the rest for the peak time and overshoot percentages. FOPID has the worst overshoot percentage, whereas the PID controller has the worst peak time characteristic. However, PID controller does perform better than the COPID for settling time. In the current study, control signals correspond to feed rate manipulation in the actual machining systems. High overshoots in feed rate settings may lead to cutting tool damage / breakage, machine tool chatter and possible safety hazard for the machinist. Therefore, minimisation of peak overshoots in feed rate manipulation is a critical machining requirement being fulfilled by the complex order PID controller. Fig. 9 and 10 give visual representations of

the relative differences among the output and control signal overshoot percentages attained by the three controllers considered in the current study. Thus, the superiority of the COPID controller over others may be appreciated in light of the importance of the peak overshoot minimisation. Fig. 11 shows the Bode diagram for the complex order controller. This plot indicates that the gain and phase margin for the COPID controller is ∞ , implying that the machined composite surface roughness system is robust against variations in the system parameters. This result is crucial from the point of view of the anisotropic structure of composite materials; that lead to system variations during machining.

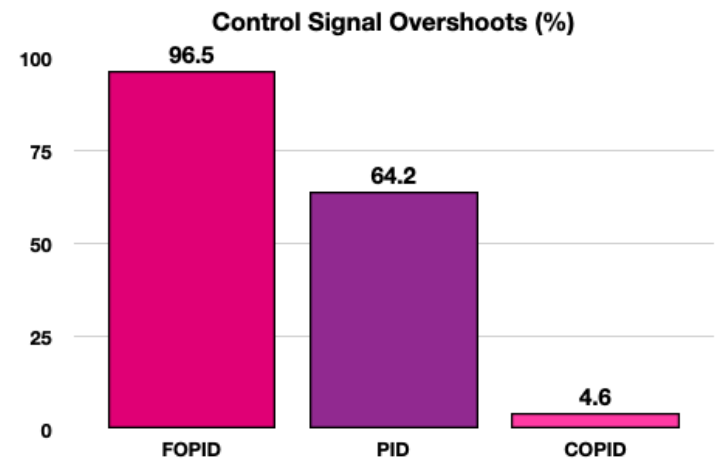


Figure 11: Control Signal Overshoots (%)

4 Conclusions

The current work is an extension of the preliminary study reported in the 2019 IEEE International Conference on Mechatronics, Robotics

and Systems Engineering (MoRSE) [1]. The preliminary study involved system identification and FOPID control of surface roughness evolution in machining of CNT Al-Mg composite materials. The ARMAX model structure controlled by the FOPID controller produced best output signal responses as reported in the maiden paper [1]. The current study expanded that work by including PID and COPID controller designs on the best performing ARMAX model structure determined in the previous work. All three controllers' responses were compared in terms of time domain specifications of the respective output and control signal responses. The current work also included analysis of the output signal trends for the said controllers (which was not considered in the preliminary study). The COPID controller conclusively demonstrated its ability to minimise and eliminate peak overshoot percentages in the control signal (feed rate) and output signal (surface roughness) responses respectively. The other two controllers (PID and FOPID) proved effective in reducing other time domain metrics viz. rise, peak and settling times. However these controllers were unable to stem the peak overshoots to minuscule levels. It is absolutely important to minimise and possibly eliminate the control/output signal overshoots to avoid the adverse affects of such overshoots on the machining process and product quality. This work establishes that the complex order PID controllers can be safely and widely adopted towards effective control of nano composite manufacturing systems for high productivity.

References

- [1] R. Sekhar, T. Singh, P. Shah, "ARX/ARMAX Modeling and Fractional Order Control of Surface Roughness in Turning Nano-Composites," in 2019 International Conference on Mechatronics, Robotics and Systems Engineering (MoRSE), 97–102, IEEE, 2019, doi:10.1109/MoRSE48060.2019.8998654.
- [2] R. Sekhar, T. Singh, "Mechanisms in turning of metal matrix composites: a review," *Journal of Materials Research and Technology*, **4**(2), 197–207, 2015, doi:https://doi.org/10.1016/j.jmrt.2014.10.013.
- [3] R. Sekhar, T. Singh, "Determination of Johnson Cook Parameters in Turning of Micro and Nano Reinforced Aluminum Composites using Trust Region Reflective Algorithm," *International Journal of Innovative Technology and Exploring Engineering*, **8**(12), 1712–1716, doi:10.35940/ijtee.L3183.1081219.
- [4] V. S. Jatti, R. Sekhar, R. Patil, "Study of ball nose end milling of LM6 al alloy: Surface roughness optimisation using genetic algorithm," *Int. J. Eng. Technol*, **5**, 2859–65, 2013, doi:http://citeseerx.ist.psu.edu/viewdoc/download?doi=10.1.1.411.1573&rep=rep1&type=pdf.
- [5] I. Podlubny, "Fractional-order systems and fractional-order controllers," *Institute of Experimental Physics, Slovak Academy of Sciences, Kosice*, **12**(3), 1–18, 1994, doi:http://people.tuke.sk/igor.podlubny/pspdf/uef0394.pdf.
- [6] R. Sekhar, T. Singh, P. Shah, "Micro and Nano Particle Composite Machining: Fractional Order Control of Surface Roughness," in Third International Conference on Powder, Granule and Bulk Solids: Innovations and Applications PGBSIA 2020 February 26-28, 2020, 35, 2020, doi:https://www.pgsbia.com/wp-content/uploads/Conference-Proceedings-PGBSIA-2020.pdf#page=40.
- [7] P. Shah, R. Sekhar, S. Agashe, "Application of Fractional PID Controller to Single and Multi-Variable Non-Minimum Phase Systems," *International Journal of Recent Technology and Engineering*, **8**(2), 2801–2811, 2019, doi:10.35940/ijrte.b2805.078219.
- [8] P. Shah, R. Sekhar, "Closed Loop System Identification of a DC Motor using Fractional Order Model," in 2019 International Conference on Mechatronics, Robotics and Systems Engineering (MoRSE), 69–74, IEEE, 2019, doi:https://doi.org/10.1109/MoRSE48060.2019.8998744.
- [9] P. Shah, S. Agashe, "Design and optimization of fractional PID controller for higher order control system," in International conference of IEEE ICART, 588–592, 2013, doi:https://www.semanticscholar.org/paper/Design-and-Optimization-of-Fractional-PID-for-Order-Shah-Agashe/6e32b76ffe9609e0423e062b8aedd87361dedd4c.
- [10] R. Bhimte, K. Bhole, P. Shah, "Fractional Order Fuzzy PID Controller for a Rotary Servo System," in 2018 2nd International Conference on Trends in Electronics and Informatics (ICOEI), 538–542, IEEE, 2018, doi:https://doi.org/10.1109/ICOEI.2018.8553867.
- [11] S. Das, *Functional fractional calculus*, Springer Science & Business Media, 2011, doi:https://doi.org/10.1007/978-3-642-20545-3.
- [12] A. Tepljakov, "FOMCON: fractional-order modeling and control toolbox," in *Fractional-order Modeling and Control of Dynamic Systems*, 107–129, Springer, 2017, doi:https://doi.org/10.1007/978-3-319-52950-9_6.
- [13] P. Shah, S. Agashe, "Design of controller for a higher order system without using model reduction methods," *Progress in Fractional Differentiation and Applications*, **3**, 289–3004, 2017, doi:http://dx.doi.org/10.18576/pfda/030405.
- [14] S. Pritesh, S. AGASHE, A. J. KULKARNI, "Design of a fractional $PI^{\lambda}D^{\mu}$ controller using the cohort intelligence method," *Frontiers of Information Technology & Electronic Engineering*, **19**(3), 437–445, 2018, doi:https://doi.org/10.1631/FITEE.1601495.
- [15] J. A. Jacob, A. V. Tare, V. A. Vyawahare, V. N. Pande, "A review of time domain, frequency domain and stability analysis of linear complex-order systems," in 2016 IEEE International WIE Conference on Electrical and Computer Engineering (WIECON-ECE), 164–169, IEEE, 2016, doi:https://doi.org/10.1109/WIECON-ECE.2016.8009110.
- [16] M. Shahiri, A. Ranjbar, M. R. Karami, R. Ghaderi, "New tuning design schemes of fractional complex-order PI controller," *Nonlinear Dynamics*, **84**(3), 1813–1835, 2016, doi:https://doi.org/10.1007/s11071-016-2608-5.
- [17] C. Li, X. Dao, P. Guo, "Fractional derivatives in complex planes," *Nonlinear Analysis: Theory, Methods & Applications*, **71**(5-6), 1857–1869, 2009, doi:https://doi.org/10.1016/j.na.2009.01.021.
- [18] J. T. Machado, "Optimal controllers with complex order derivatives," *Journal of Optimization Theory and Applications*, **156**(1), 2–12, 2013, doi:https://doi.org/10.1007/s10957-012-0169-4.
- [19] K. Khandani, A. A. Jalali, M. R. R. Mehdiabadi, "Robust complex order controller design for DC motors," in 20th Iranian Conference on Electrical Engineering (ICEE2012), 900–903, IEEE, 2012, doi:https://doi.org/10.1109/IranianCEE.2012.6292481.
- [20] C. M. Pinto, A. R. Carvalho, "Effect of drug-resistance in a fractional complex-order model for HIV infection," *IFAC-PapersOnLine*, **48**(1), 188–189, 2015, doi:https://doi.org/10.1016/j.ifacol.2015.05.162.
- [21] A. Guefrachi, S. Najjar, M. Amairi, M. Aoun, "Tuning of fractional complex order PID controller," *IFAC-PapersOnLine*, **50**(1), 14563–14568, 2017, doi:https://doi.org/10.1016/j.ifacol.2017.08.2093.
- [22] O. Hanif, G. B. Babu, S. Sharma, "Performance Improvement of $PI^{\lambda+iy}D^{\mu}$ Fractional Complex Order Controller using Genetic Algorithm," in 2018 Fourth International Conference on Advances in Electrical, Electronics, Information, Communication and Bio-Informatics (AEEICB), 1–5, IEEE, 2018, doi:https://doi.org/10.1109/AEEICB.2018.8480981.
- [23] M. F. Silva, J. T. Machado, R. S. Barbosa, "Complex-order dynamics in hexapod locomotion," *Signal processing*, **86**(10), 2785–2793, 2006, doi:https://doi.org/10.1016/j.sigpro.2006.02.024.
- [24] A. V. Tare, J. A. Jacob, V. A. Vyawahare, V. N. Pande, "Design of novel optimal complex-order controllers for systems with fractional-order dynamics," *International Journal of Dynamics and Control*, **7**(1), 355–367, 2019, doi:https://doi.org/10.1007/s40435-018-0448-5.
- [25] J. L. Adams, T. T. Hartley, L. I. Adams, "A solution to the fundamental linear complex-order differential equation," *Advances in Engineering Software*, **41**(1), 70–74, 2010, doi:https://doi.org/10.1016/j.advengsoft.2008.12.014.

- [26] M. Shahiri, A. Ranjbar, M. R. Karami, R. Ghaderi, "Robust control of non-linear PEMFC against uncertainty using fractional complex order control," *Nonlinear Dynamics*, **80**(4), 1785–1800, 2015, doi:<https://doi.org/10.1007/s11071-014-1718-1>.
- [27] K. J. Åström, P. Eykhoff, "System identification—a survey," *Automatica*, **7**(2), 123–162, 1971, doi:[https://doi.org/10.1016/0005-1098\(71\)90059-8](https://doi.org/10.1016/0005-1098(71)90059-8).
- [28] P. Shah, S. Agashe, "Review of fractional PID controller," *Mechatronics*, **38**, 29–41, 2016, doi:<https://doi.org/10.1016/j.mechatronics.2016.06.005>.
- [29] P. Shah, S. Agashe, "Experimental Analysis of Fractional PID Controller Parameters on Time Domain Specifications," *Progress in Fractional Differentiation and Applications*, **3**, 141–154, 2017, doi:<http://dx.doi.org/10.18576/pfda/030205>.
- [30] P. Lanusse, A. Oustaloup, B. Mathieu, "Third generation CRONE control," in *Proceedings of IEEE Systems Man and Cybernetics Conference-SMC*, **2**, 149–155, IEEE, 1993, doi:<https://doi.org/10.1109/ICSMC.1993.384864>.
- [31] K. H. Ang, G. Chong, Y. Li, "PID control system analysis, design, and technology," *IEEE transactions on control systems technology*, **13**(4), 559–576, 2005, doi:<https://doi.org/10.1109/TCST.2005.847331>.